DYRK1A-mediated PLK2 phosphorylation regulates the proliferation and invasion of glioblastoma cells

SHICHUAN TAN[1-3], JUAN ZHAO[1] and PIN WANG[1]

[1]Department of Otorhinolaryngology, Qilu Hospital of Shandong University, National Health Commission (NHC) Key Laboratory of Otorhinolaryngology, Shandong University; [2]Department of Emergency Neurosurgical Intensive Care Unit, Qilu Hospital of Shandong University; [3]Department of Neurosurgery, Qilu Hospital and Institute of Brain and Brain-Inspired Science, Cheeloo College of Medicine, Shandong University, Jinan, Shandong 250012, P.R. China

Received March 28, 2023; Accepted June 13, 2023

DOI: 10.3892/ijo.2023.5542

Abstract. Polo-like kinases (PLKs) are a family of serine-threonine kinases that exert regulatory effects on diverse cellular processes. Dysregulation of PLKs has been implicated in multiple cancers, including glioblastoma (GBM). Notably, PLK2 expression in GBM tumor tissue is lower than that in normal brains. Notably, high PLK2 expression is significantly correlated with poor prognosis. Thus, it can be inferred that PLK2 expression alone may not be sufficient for accurate prognosis evaluation, and there are unknown mechanisms underlying PLK2 regulation. In the present study, it was demonstrated that dual specificity tyrosine-phosphorylation-regulated kinase 1A (DYRK1A) interacts with and phosphorylates PLK2 at Ser358. DYRK1A-mediated phosphorylation of PLK2 increases its protein stability. Moreover, PLK2 kinase activity was markedly induced by DYRK1A, which was exemplified by the upregulation of alpha-synuclein S129 phosphorylation. Furthermore, it was found that phosphorylation of PLK2 by DYRK1A contributes to the proliferation, migration and invasion of GBM cells. DYRK1A further enhances the inhibition of the malignancy of GBM cells already induced by PLK2. The findings of the present study indicate that PLK2 may play a crucial role in GBM pathogenesis partially in a DYRK1A-dependent manner, suggesting that PLK2 Ser358 may serve as a therapeutic target for GBM.

Correspondence to: Dr Pin Wang, Department of Otorhinolaryngology, Qilu Hospital of Shandong University, National Health Commission (NHC) Key Laboratory of Otorhinolaryngology, Shandong University, 44 Wenhuaxi Road, Jinan, Shandong 250012, P.R. China
E-mail: wangpin@sdu.edu.cn

Key words: glioblastoma, polo-like kinase 2, dual specificity tyrosine-phosphorylation-regulated kinase 1A, phosphorylation, tumor metastasis

Introduction

Gliomas are tumors arising within the brain and the spinal cord, among which glioblastoma (GBM) is widely acknowledged as the most malignant tumor (1). Despite significant advances in understanding of GBM tumorigenesis and treatment over the past few decades, patients with GBM continue to face dismal outcomes, characterized by high recurrence rates and rapid disease progression (2). Therefore, it is imperative to further explore the underlying mechanisms of GBM pathogenesis to improve patient prognosis.

Therapeutics targeting kinases have shown promise as an efficacious treatment for a variety of cancers, given the high correlation between those kinases and the initiation and progression of certain cancers (3). To date, several kinase inhibitors have been approved by the U.S. Food and Drug Administration for clinical use in cancer treatment (4,5). Polo-like kinases (PLKs) comprise a protein family that selectively binds to and phosphorylates substrates on specific motifs recognized by the POLO box domains. The PLK family consists of five members, among which PLK2 has been implicated as a potential tumor suppressor. PLK2 downregulation has been observed in several types of cancers, including breast cancer, GBM, HPV^+ head and neck squamous cell carcinoma, kidney chromophobe, lung adenocarcinoma, lung squamous cell carcinoma, prostate adenocarcinoma and uterine corpus endometrial carcinoma. However, PLK2 upregulation has also been detected in cholangiocarcinoma, colon adenocarcinoma, esophageal carcinoma, kidney renal clear cell, kidney renal papillary cell carcinoma, pheochromocytoma and paraganglioma, stomach adenocarcinoma and thyroid cancer on TIMER2.0 (Fig. 1A; http://timer.cistrome.org/). These data indicate multifaceted roles of PLK2 in different cancers. Furthermore, recent findings have identified PLK2 as a novel biomarker for the prognosis of human GBM (6). The PLK2/Notch axis may be closely linked to the development of acquired resistance to temozolomide in GBM (7). Consequently, further investigation is necessary to comprehensively understand the role of PLK2 in GBM tumorigenesis.

Dual specificity tyrosine-phosphorylation-regulated kinases (DYRKs) constitute a group of evolutionarily conserved kinases that induce phosphorylation on tyrosine,

serine and threonine residues. A total of five members have been identified, including DYRK1A, DYRK1B, DYRK2, DYRK3 and DYRK4. DYRKs are known to phosphorylate a broad range of proteins involved in diverse cellular processes (8). Abnormal expression or activity of DYRK1A has been implicated in the development of numerous cancers, including B-cell acute lymphoblastic leukemia, hepatocellular carcinoma and glioma (9-11). DYRK1A inhibitors have been approved for the treatment of certain types of cancer, such as metastatic breast cancer (12). The role of DYRK1A is complex, and whether DYRK1A employs tumor suppressive or oncogenic activities is most likely dependent on its specific substrates. For instance, DYRK1A exerts a tumor-promoting effect by phosphorylating various transcription factors, including Gli1 and STAT3 (13,14). Conversely, DYRK1A may maintain its antitumor effect by activating ASK1 (15). The precise role of DYRK1A in GBM pathogenesis has yet to be fully elucidated. In the present study, it was demonstrated that DYRK1A phosphorylates PLK2 at Ser358. DYRK1A-mediated phosphorylation of PLK2 enhances both protein stability and kinase activity. Introduction of PLK2 leads to a significant decrease in glioma cell malignancy, which is further weakened in the presence of DYRK1A. These results suggested a potential contribution of DYRK1A-mediated PLK2 phosphorylation to glioma pathogenesis.

Materials and methods

Dataset acquisition. The transcriptome sequencing data and corresponding clinical data of primary GBM were procured from The Cancer Genome Atlas (TCGA) database (https://portal.gdc.cancer.gov/). The present study utilized the TCGA GBM cohort comprising 169 tumor samples and 5 normal brain samples to analyze differentially expressed genes (DEGs) using count data. Additionally, PLK2 expression across cancers was evaluated using the TIMER2.0 website. The GSE68848, GSE16011 and GSE4290 datasets downloaded from the Gene Expression Omnibus database (GEO; https://www.ncbi.nlm.nih.gov/geo/) were employed to further validate the expression of PLK2 (16-18). Overall survival (OS) information was also acquired from the datasets for prognostic evaluation. Clustal Omega (https://www.ebi.ac.uk/Tools/msa/clustalo/) was used for multiple sequence alignment.

Identification of differentially expressed genes and function analysis. Differentially expressed genes were identified as previously described (19). DEGs between GBM tissues and normal brain tissues were analyzed using the 'limma', 'edgeR' and 'DESeq2' R packages with the cutoff criteria of $|\log2FC|\geq1$ and $P<0.05$. The raw count data of the TCGA GBM cohort were employed as the input for limma, edgeR and DESeq2. Volcano plots were generated to display DEG distribution from the three algorithms mentioned above with the 'tinyarray' R package. Gene Ontology (GO) and Kyoto Encyclopedia of Genes and Genomes (KEGG) analyses were performed utilizing the 'clusterProfiler' R package to predict the biological functions and related pathways. Kaplan-Meier analysis to assess the overall survival of patients was performed with 'survminer' and 'survival' R packages. Log-rank test was used to compare the survival curves between the groups.

Cell culture, vectors and transfection. The human cell lines 293 (cat. no. CRL-1573), 293T (cat. no. CRL-3216) and U87MG (cat. no. HTB-14) were obtained from the American Type Culture Collection (ATCC). Of note, U87MG cells were cells established likely from GBM of unknown origin. U251MG cells were purchased from Cell Bank Type Culture Collection, Chinese Academy of Sciences (Xi'an China) as previously described (20). 293, 293T, U87MG and U251MG cells were cultured in high glucose DMEM supplemented with 10% FBS, 100 units/ml penicillin and 0.1 mg/ml streptomycin. All cells were maintained in a 37˚C humidified incubator containing 5% CO_2. All experiments were performed using cells within 20 passages after receipt.

For transfection, cells were seeded into cell culture dishes or plates. When cell confluency reached ~80% within 24 h, plasmids were transfected into cells by Lipofectamine 3000 transfection reagent at room temperature (for six-well plate, 2.5 μg plasmid in total was used in transfection for each well). All transfections were carried out with Lipofectamine 3000 (cat. no. L3000001; Thermo Fisher Scientific, Inc.) according to the manufacturer's instructions.

Expression plasmids were generated by inserting the gene of interest into pCMV6-entry and pcDNA3.1+ C-HA. pCMV6-entry and pcDNA3.1+ C-HA were purchased from OriGene Technologies, Inc. (cat. no. PS100001) and Addgene, Inc. (plasmid cat. no. 128034), respectively. DYRK1A (K179R), PLK2S248A, and PLK2S358A mutant-expressing plasmids generated by inserting specific sequences into the pCMV6-entry vector were purchased from Charles River Laboratories, Inc. pCMV6-entry and pcDNA3.1+ C-HA were used as negative control vectors in transfection.

Cycloheximide (CHX) chase assay. Cycloheximide was purchased from MedChemExpress (cat. no. HY-12320). A CHX chase assay was performed as previously described (21). Briefly, 293 cells were seeded in six-well plates one day before transfection. 293 cells were transfected according to the manufacturer's instructions. A total of 36 h after transfection, cells were treated with 150 μg/ml CHX and separately harvested at 0, 1, 2, 4, 6, and 8 h for western blotting (WB).

Cell proliferation and viability assay. Cell Counting Kit-8 (WST-8/CCK-8) (cat. no. C0043; Beyotime Institute of Biotechnology) was used as a convenient and robust way of performing a cell viability assay. Briefly, cells were suspended adequately and seeded into 96-well plates at a density of $5x10^3$ cells/well with 3 replicates a day before the cell viability assay was performed as follows: The supernatant was removed, and 100 μl fresh medium containing 10% CCK-8 reagent was added as a working solution at 0, 24, 48, and 72 h time points. The OD450 and OD650 values of each well were measured by a microplate reader after the cells were incubated with working solution for 1.5 h in a 37˚C humidified incubator containing 5% CO_2.

Transwell invasion assay. Transwell plates (8-μm diameter pores; Corning, Inc.) were used to determine the invasion potential of U87MG and U251MG cells. Briefly, the upper faces of the membranes were precoated with Matrigel (cat no. 354234; BD Biosciences) at 37˚C for 1 h. A total of

$5x10^4$ cells were resuspended in serum-free medium and transferred into the upper chambers in triplicate. Complete cell culture media were added to the lower chambers. After 60 h of incubation at 37˚C humidified incubator containing 5% CO_2, the media were removed, and the cells were fixed with 4% paraformaldehyde for 20 min at room temperature. A 0.1% (w/v) crystal violet solution was used for cell staining. The upper side of the filter was gently wiped with cotton swabs, and the chamber was air-dried. Representative images were captured by inverted microscopy. The total number of cells on ten individual fields for each membrane was counted; average numbers and standard deviation of invading cells were calculated.

Wound healing assay. U251MG and U87MG cells were seeded on a six-well plate and cultured until the cell confluence reached ~90%. Straight line wounds were created by scratching a cell monolayer with sterile 100-μl pipette tips. The medium was gently replaced for the removal of the non-adherent cells generated during scratching. Cells were then maintained in serum-free media. The cells migrated slowly to fill the wound area. Images of the wells were captured at 0 and 48 h, separately. Wound areas were used to assess the migration rate of the cells. The results were quantified and analyzed using ImageJ 1.53t software (National Institutes of Health).

mRNA extraction and reverse transcription-quantitative (RT-q) PCR. Total RNA was extracted from cells by TRI Reagent following the manufacturer's instructions (cat. no. T9424; Sigma-Aldrich; Merck KGaA). Reverse transcription was performed using the PrimeScript™ RT reagent kit with gDNA eraser (cat no. RR047A; Takara Bio, Inc.). RT-qPCR assays were performed as previously described (22). cDNA was synthesized from 1 μg of total RNA by HiScript III RT SuperMix (cat. no. R323-01; Vazyme Biotech Co., Ltd.). qPCR was performed using a LightCycler480II Real-time PCR system [Roche Diagnostics (Shanghai) Co., Ltd.] with SYBR® Green-based gene expression analysis. A comparative CT method ($2^{-\Delta\Delta Cq}$) was used to analyze the gene expression level as previously described (23). The primers targeting PLK2 for qPCR were as follows: forward, 5'-CTACGCCGCAAAAATTATTCC TC-3' and reverse, 5'-TCTTTGTCCTCGAAGTAGTGG T-3'. The internal control of qPCR was beta-actin, with the following primers: forward, 5'-GACAGGATGCAGAAG GAGATTACT-3' and reverse, 5'-TGATCCACATCTGCT GGAAGGT-3'.

Colony formation assay. The colony formation assay is an *in vitro* cell survival assay that is used to evaluate the ability of a single cell to grow into a colony. The colony is defined to consist of at least 50 cells (24). U251MG cells were counted and seeded at $8x10^2$ cells per six-cm plate. Media were changed every four days. After two weeks, cell colonies were grown, and the media were removed. Cells were washed with PBS three times, fixed with 4% paraformaldehyde for 15 min at room temperature, and stained with 0.1% crystal violet for 30 min. The colonies were counted manually under a microscope and images were captured.

Immunofluorescence. U251MG cells were fixed with 4% paraformaldehyde at room temperature for 20 min and immunostained with mouse anti-DYRK1A (cat. no. WH0001859M1; MilliporeSigma) at a dilution of 1:100 and rabbit anti-PLK2 sequentially at a dilution of 1:100 (cat. no. 14812; Cell Signaling Technology, Inc.). CoraLite488-conjugated goat anti-rabbit IgG (H+L) (SA00013-2) and CoraLite594-conjugated goat anti-mouse IgG (H+L) (cat. no. SA00013-3; Proteintech Group, Inc.) were used to index and display the immunofluorescent signals both at a dilution of 1:200. DAPI (1 μg/ml; Roche Applied Science) was applied in mounting medium to indicate the nucleus. The images were captured by a fluorescence confocal microscope (LSM880; Leica Microsystems GmbH). The association analysis was achieved by ImageJ 1.53t software.

WB, antibodies, and reagents. Cells were harvested and washed with ice-cold PBS twice. RIPA lysis buffer (Beyotime Institute of Biotechnology) mixed with a protease inhibitor cocktail mixture was used for cell lysis. The protein concentration was determined by a Pierce™ BCA Protein Assay kit. Protein samples were separated by 10 and 12% glycine SDS-PAGE. PageRuler pre-stained protein ladder (Thermo Fisher Scientific, Inc.) was used to indicate protein molecular weights. Proteins were transferred from the gel to nitrocellulose membranes. The membranes were blocked with 5% non-fat milk (in 1X Tris-buffered saline with 0.1% Tween®20) at room temperature for 1 h. The primary antibodies used in the present study were as follows: anti-FLAG antibody (cat. no. F1804; MilliporeSigma), HA-Tag antibody (F-7) (cat. no. sc-7392; Santa Cruz Biotechnology, Inc.), anti-DYRK1A antibody (7D10) (cat. no. WH0001859M1; MilliporeSigma), anti-GAPDH antibody (cat. no. 60004-1-Ig; Proteintech Group, Inc.), anti-β-actin antibody (cat. no. A1978; MilliporeSigma), anti-PLK2 antibody (cat. no. 14812; Cell Signaling Technology, Inc.), p-Ser/Phosphoserine antibody (cat. no. sc-81514, Santa Cruz Biotechnology, Inc.), anti-alpha-synuclein antibody (cat. no. 66412-1-Ig; Cell Signaling Technology, Inc.) and anti-alpha-synuclein (phospho S129) antibody (cat. no. ab51253; Abcam). Secondary antibodies IRDye®680RD goat anti-mouse IgG (cat. no. 926-68070), IRDye®680RD goat anti-rabbit IgG (cat. no. 926-68071), IRDye®800CW goat anti-mouse IgG (cat. no. 926-32210) and IRDye®800CW goat anti-rabbit IgG (cat. no. 926-32211) were all purchased from LI-COR Biosciences. Images were acquired by directly scanning the nitrocellulose membranes with LI-COR Odyssey classic imager from LI-COR Biosciences-U.S. The quantification was performed by ImageJ 1.53t software. Harmine was purchased from MedChemExpress (cat. no. HY-N0737A).

Coimmunoprecipitation assay. Coimmunoprecipitation assays were performed as previously described (22). Briefly, cells were harvested and lysed in WB and IP cell lysis buffer containing 20 mM Tris (pH 7.5), 150 mM NaCl, and 1% Triton X-100 in the presence of a protease inhibitor mixture (Roche Applied Science). The cell lysate was centrifuged at 22,000 x g at 4˚C for 15 min. The supernatant was carefully retained. Supernatant containing 100 μg protein was saved and used as input. Primary antibodies and protein A/G-agarose beads (Santa Cruz Biotechnology, Inc.) were added to the

supernatant and maintained on a tube rotator at 4˚C for 4 h. Mouse IgG (Beyotime Institute of Biotechnology) was applied as a negative control. Samples were analyzed by 10% glycine SDS-PAGE.

Lentivirus production and transduction. The lentivirus vectors were prepared based on the 2nd generation system. Lentiviruses were produced by transfection of 293T cells with three plasmids together, pLent-EF1a-FH-CMV-Puro (pLV100008-OE; WZ Biosciences) carrying the gene of interest, pMD2. G (cat. no. 12259; Addgene, Inc.), and psPAX2 (cat. no. 12260; Addgene, Inc.) packaging constructs. 293T cells were plated in 100-mm dishes to reach 70-90% confluency by the time of transfection. The transfection was performed at room temperature with the vectors of pLent-EF1a-FH-CMV-Puro (10 μg), pMD2. G (5 μg) and psPAX2 (10 μg) for each 100-mm cell culture dish. Media were refreshed after 12 h of transfection (10 ml for each 100-mm dish). A total of 48 h after transfection, the lentivirus-containing supernatant was collected and filtered with 0.45 μm filters to isolate the lentiviral particles for the following infection. These lentiviruses were introduced into U87MG and U251MG cell lines on Day 2 of culture at a volume ratio of 1:5. The cell culture media were replaced with fresh media within 24 h of infection and incubated for 5 days before further experiments. Stable clones transduced with PLK2, DYRK1A, shPLK2 and scramble control were selected for 10 days by puromycin at the concentration of 2 μg/ml. Lentiviral particles packaging human PLK2 and DYRK1A are based on the sequences of Q9NYY3 and Q13627-2, respectively, in the UniProt database (https://www.uniprot.org/). Lentiviral particles packaging the shRNA targeted PLK2 (5'-TAGTCAAGTGACGGTGCTG-3') and the scramble control (5'-TTCTCCGAACGTGTCACGT-3').

Dephosphorylation assay. Cell lysate samples containing 100 μg protein were incubated with thermosensitive alkaline phosphatase (AP; cat. no. EF0651; Thermo Fisher Scientific, Inc.) at 37˚C for 30 min. Then, the sample was placed into a 75˚C metal bath for 5 min to deactivate AP. Samples were analyzed by WB.

Statistical analysis. Data are presented as the mean ± standard deviation (SD) from three independent experiments. For immunoblotting, one representative picture is shown. Quantifications from three independent experiments are defined with blot density by ImageJ 1.53t software. Differences between two groups are determined by unpaired Student's t-test. Two-way ANOVA followed by Tukey's post hoc test was applied for multiple comparisons of the protein level change at different time point for CHX assay. The data are evaluated for statistical significance with analysis of variance or non-parametric analysis by Prism 7 (Dotmatics). $P<0.05$ was considered to indicate a statistically significant difference.

Results

PLK2 is downregulated in GBM and significantly associated with prognosis. PLK2 exhibits widespread dysregulation across multiple cancer types. The expression of PLK2 in tumors and normal tissues was explored on TIMER2.0 (Fig. 1A). To improve understanding of the expression of PLK2 in GBM, three differential expression analyses were conducted between tumor tissues and normal brains in the TCGA-GBM cohort. DEGs in the TCGA-GBM cohort were visualized using Volcano plots (Fig. 1B). As indicated, PLK2 was markedly downregulated in GBM tissues compared with normal brains (Fig. 1B and C). The downregulation of PLK2 in tumor tissues was further confirmed in the GSE68848 and GSE4290 datasets (Fig. 1D and E, respectively). In addition, PLK2 expression was considered to be associated with the OS of GBM patients (6). Function analysis was performed with common upregulated and downregulated genes (Fig. S1). GO analysis suggested that features relevant to tumor malignancy are promoted, such as positive regulation of cell adhesion, focal adhesion and extracellular matrix structural constituent (Fig. S1A). KEGG analysis revealed upregulation of classic pathways associated with tumor growth, including ECM-receptor interaction, cell adhesion molecules, and transcriptional misregulation in cancer (Fig. S1B). Kaplan-Meier analysis followed by the log-rank test was performed to assess OS. The OS of patients evidently exhibited that high expression of PLK2 was strongly associated with poor prognosis in both the TCGA-GBM cohort and GSE16011 dataset (Fig. 1F and G). It should be noted that PLK2 expression is lower in tumor tissues, but low PLK2 expression predicts favorable prognosis. Due to the inconsistency of PLK2 expression and prognosis value, pathways and functions predicted by function analysis may not be markedly suggestive. This seemingly paradoxical finding suggests that other unidentified mechanisms may regulate PLK2 in GMB pathogenesis, warranting further investigation.

DYRK1A modulates PLK2 protein levels in a kinase activity-dependent manner. PLK2 is mainly involved in cellular biofunctions by direct phosphorylation of specific substrates. However, the critical role of phosphorylation in its kinase activity remains poorly understood (25). Endogenous PLK2 protein in 293 cells is extremely low and could be barely detected by WB. Hence, 293 cells were only used for detection of exogenous PLK2 after transfection. In the present study, DYRK1A and PLK2 expression vectors were transfected into 293 cells and it was found that overexpression of DYRK1A led to a significant increase in exogenous PLK2 protein levels by ~5.6-fold compared with the control, while PLK2 mRNA levels remained relatively unchanged (Fig. 2A and B). To confirm that endogenous PLK2 protein is also regulated by DYRK1A, a DYRK1A-expressing vector was transfected into two GBM cell lines. The results revealed that PLK2 protein levels were increased to 180±1.0 and 147±1.3% upon DYRK1A overexpression compared with the controls in U87MG cells and U251MG cells, respectively (Fig. 2C and E). Meanwhile, PLK2 mRNA was relatively unchanged upon DYRK1A overexpression in both cell lines (Fig. 2D and F). These results suggested that DYRK1A likely exerts post-translational regulation on PLK2. As a protein kinase, DYRK1A is commonly involved in cellular processes by phosphorylation on specific substrates. It was then explored whether PLK2 is phosphorylated by DYRK1A. As expected, the phosphorylation and total levels of PLK2 were both upregulated in the presence of DYRK1A (Fig. 2G). DYRK1A-mediated PLK2 phosphorylation was mostly eliminated by treatment with AP (Fig. 2H). A previous study found that the substituted mutant with Arg in place of

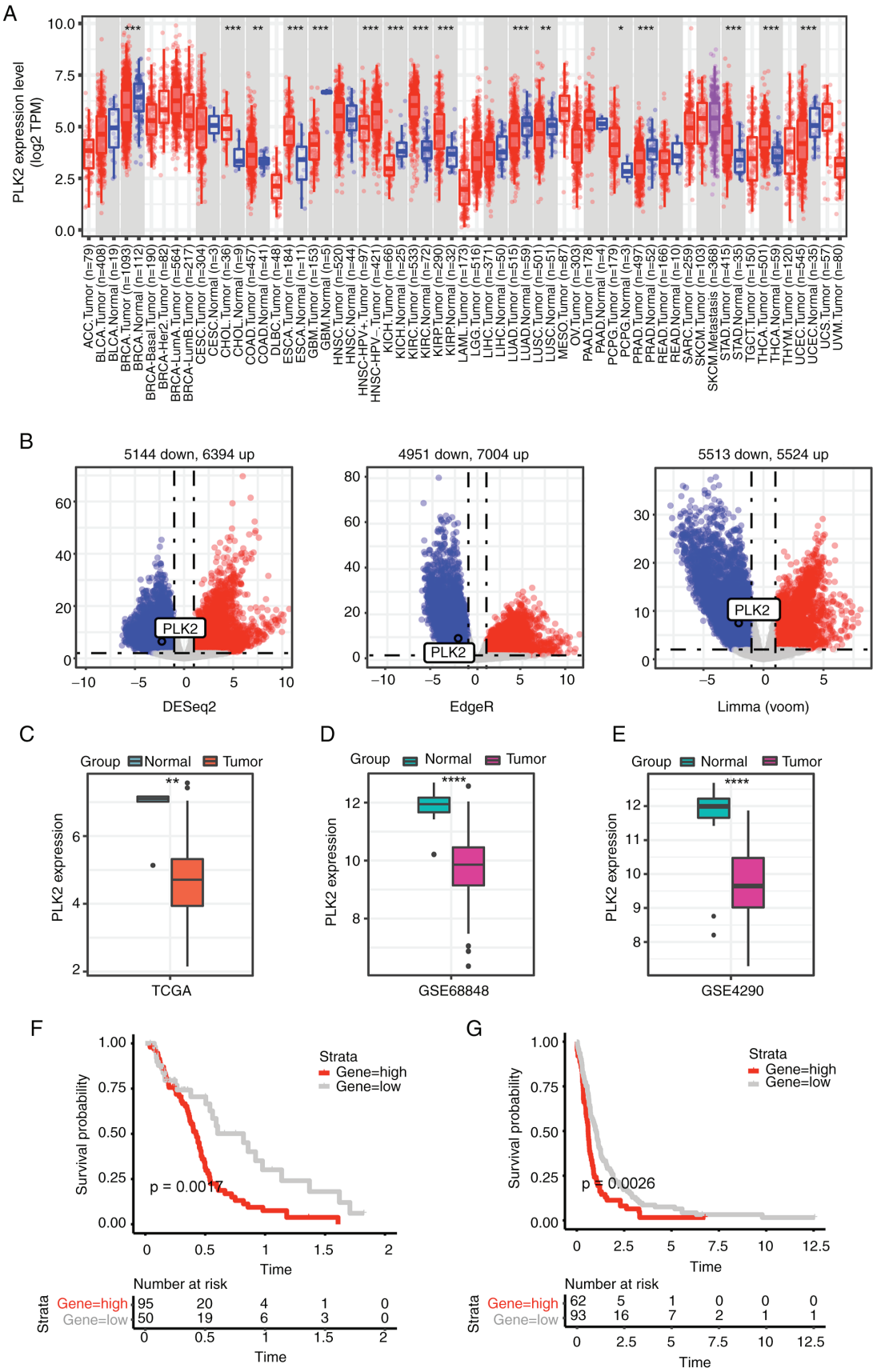

Figure 1. PLK2 is differentially expressed in GBM and is significantly associated with prognosis. (A) PLK2 expression analyzed in tumors and corresponding normal tissues in the TIMER2.0 database. (B) Volcano plot of differentially expressed genes between 169 GBM samples and 5 normal brain samples identified by edgeR, limma, and DESeq2 algorithms with the cutoff criterion P<0.05 and |log2FC|≥1. Blue dots: significantly downregulated genes; red dots: significantly upregulated genes. PLK2 is indicated by a black circle in the diagrams. (C-E) PLK2 expression in GBM tumors and normal brains in the (C) TCGA cohort, (D) GSE68848 dataset and (E) GSE4290 dataset. (F) Kaplan-Meier survival analysis of PLK2 high (red line) and low (gray line) expression groups in the TCGA cohort. (G) Kaplan-Meier survival analysis of PLK2 high (red line) and low (gray line) expression groups in the Gene Expression Omnibus cohort (GSE16011). *P<0.05, **P<0.01, ***P<0.001, and ****P<0.0001. PLK2, polo-like kinase 2; GBM, glioblastoma; TCGA, The Cancer Genome Atlas.

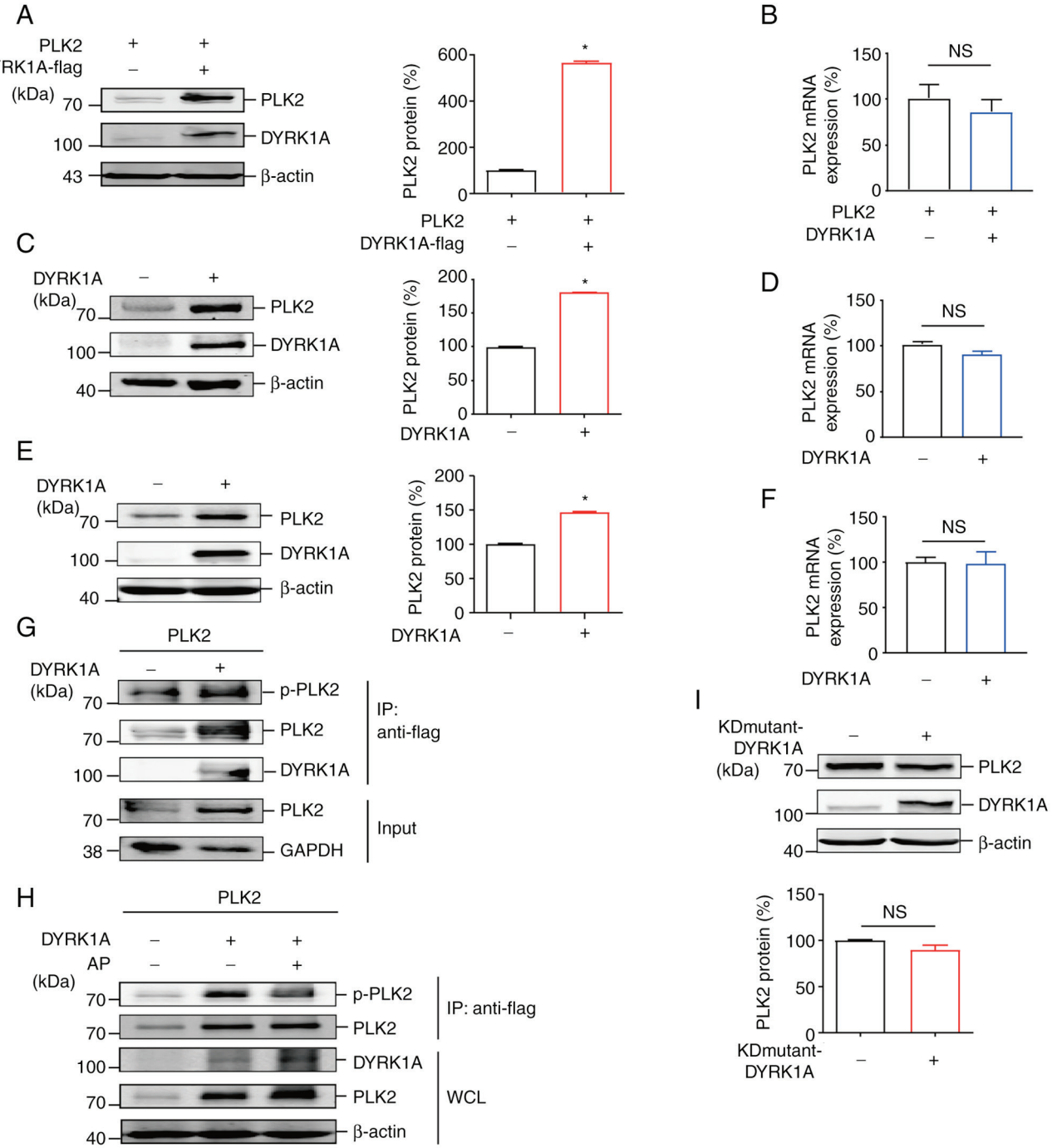

Figure 2. DYRK1A modulates PLK2 protein levels in a kinase activity-dependent manner. (A) 293 cells were cotransfected with the PLK2 expression vector together with the DYRK1A expression vector or the control vector. PLK2 and DYRK1A were detected by anti-Flag antibody and anti-DYRK1A antibody, respectively (n=3). (B) Cells and transfection conditions were the same as in panel A. RNA was isolated 48 h after transfection. RT-qPCR was performed to examine PLK2 mRNA expression (n=3). Results were normalized to the control group. (C and E) (C) U87MG and (E) U251MG cells were transfected with the DYRK1A expression vector or the control vector. PLK2 and DYRK1A proteins were examined. (D and F) Cells and transfection conditions were the same as in panels C and E. PLK2 mRNA expression in (D) U87MG and (F) U251MG cells was detected by RT-qPCR (n=3). (G) Co-immunoprecipitation was performed on 293 cells transfected with PLK2 and DYRK1A/control expression vectors. p-PLK2, PLK2, and DYRK1A were detected by WB (n=3). (H) A dephosphorylation assay was performed on 293 cells transfected with PLK2 and DYRK1A expression vectors. PLK2 was pulled down by immunoprecipitation with an anti-Flag antibody and blotted with an anti-p-Ser antibody. Cell lysates were maintained with alkaline phosphatase at 37˚C for 30 min for dephosphorylation. p-PLK2, PLK2, and DYRK1A were detected by WB (n=3). (I) U87MG cells were transfected with a kinase-dead mutant of DYRK1A (K179R) and the control vector. Endogenous PLK2 and DYRK1A proteins were examined by WB (n=3). *P<0.05. DYRK1A, dual specificity tyrosine-phosphorylation-regulated kinase 1A; PLK2, polo-like kinase 2; RT-qPCR, reverse transcription-quantitative PCR; WB, western blotting; p-, phosphorylated; NS, not significant.

Lys179 (K179R) in DYRK1A disrupts the direct interaction with ATP. The K179R mutant of DYRK1A is kinase-inactive, and its autophosphorylation ability is impaired (26). To further validate that the kinase activity of DYRK1A is essential for PLK2 phosphorylation, the DYRK1A kinase inactive K179R mutant vector was transfected into U87MG cells. In contrast to wild-type DYRK1A, the DYRK1A K179R mutant failed to induce PLK2 protein accumulation (Fig. 2I). These results

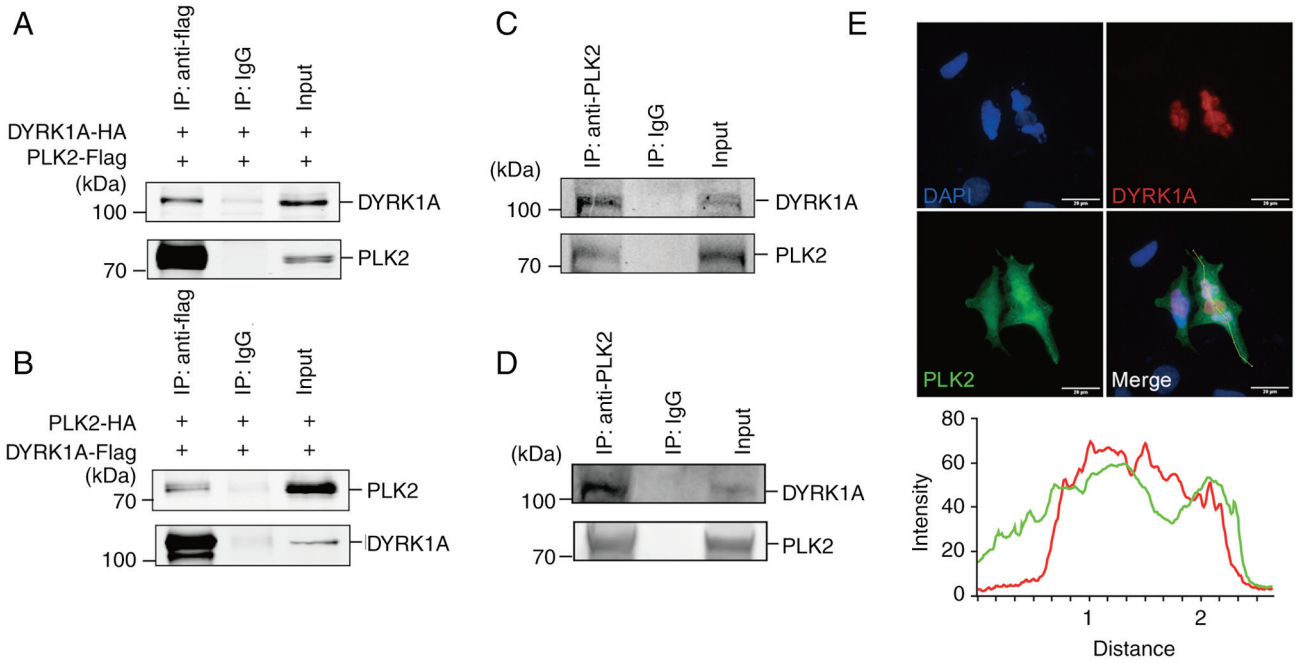

Figure 3. DYRK1A interacts with PLK2 in glioma cells. (A) Co-immunoprecipitation was performed on 293 cells transfected with DYRK1A-HA and PLK2-Flag vectors to evaluate the interaction of PLK2 and DYRK1A. Anti-Flag antibody was used for protein pull-down. HA-Tag antibody was used for WB. (B) Co-immunoprecipitation was performed on 293 cells transfected with DYRK1A-Flag and PLK2-HA vectors. Antibodies for protein pull-down and WB were the same as in A. (C and D) Co-immunoprecipitation was performed on (C) U87MG and (D) U251MG cells. An anti-ti-PLK2 antibody was used for protein pull-down. DYRK1A was detected by WB. (E) Immunofluorescence of U251MG cells was performed to determine their binding. Confocal microscopy was used to acquire images. Colocalization analysis of endogenous DYRK1A and PLK2 was achieved by ImageJ software. DYRK1A, dual specificity tyrosine-phosphorylation-regulated kinase 1A; PLK2, polo-like kinase 2; WB, western blotting.

demonstrated that DYRK1A increases PLK2 protein levels in a kinase activity-dependent manner by directly phosphorylating PLK2.

DYRK1A interacts with PLK2 in glioma cells. To validate whether DYRK1A directly interacts with PLK2, co-immunoprecipitation was employed. The results demonstrated that PLK2 can pull down DYRK1A in 293 cells (Fig. 3A). Similarly, DYRK1A was able to pull down PLK2 as well (Fig. 3B). To further explore the interaction of endogenous DYRK1A and PLK2, co-immunoprecipitation was performed in U87MG and U251MG cells. A significant interaction between DYRK1A and PLK2 was observed in both cell lines (Fig. 3C and D). Immunofluorescence was then performed to confirm the intracellular localization of DYRK1A and PLK2. PLK2 scattered in both the nucleus and cytoplasm, while DYRK1A mainly stayed in the nucleus (Fig. 3E). Colocalization analysis showed that they were predominantly colocalized in the U251MG cell nucleus.

Identification of phosphorylation sites in PLK2 by DYRK1A. It was previously found that a large proportion of DYRK1A-recognized substrates contain a consensus RPX(S/T)P motif (27). To identify the potential phosphorylation sites on PLK2, sequence alignment with RPX(S/T)P was performed using the Clustal Omega alignment tool (https://www.ebi.ac.uk/Tools/msa/clustalo/). As shown in Fig. 4A, two highly conserved sites, Ser248 and Ser358, were revealed in the PLK2 coding region. Substituted mutants of PLK2 S248A and S358A were constructed and employed to further validate whether Ser248 and Ser358 are phosphorylated by DYRK1A. The results revealed that, consistent with wild-type PLK2, PLK2 S248A mutant protein was significantly increased by DYRK1A. However, the PLK2 Ser358A mutant had only a mild increase upon DYRK1A overexpression (Fig. 4B and C). These results indicated that Ser358 in PLK2 may be the phosphorylation site induced by DYRK1A.

Phosphorylation at Ser358 increases PLK2 protein stability. The impact of phosphorylation on protein stability is an important regulatory mechanism of post-translational modifications. To explore whether phosphorylation of PLK2 induced by DYRK1A affects its protein stability, a CHX assay was conducted. A previous study revealed that PLK2 is degraded rapidly, with a half-life of ~15 min (28). Nevertheless, in the present study it was demonstrated that PLK2 protein is still detectable even after treatment with CHX for 8 h. Within 8 h, degradation of PLK2 was significantly slower in the presence of DYRK1A than in the control (Fig. 5A). Similarly, the phosphorylation-mimicking mutant PLK2S358D also exhibited decelerated degradation compared with wild-type PLK2. By contrast, PLK2S358A manifests remarkably accelerated degradation. These data demonstrated that DYRK1A-mediated PLK2 phosphorylation plays a crucial role in regulating PLK2 protein stability. Harmine is a potent and selective natural DYRK inhibitor that is commonly applied to deactivate DYRK1A kinase activity (29,30). Harmine was employed to further validate whether DYRK1A kinase activity is vital for PLK2 protein stability. The results revealed that treatment with harmine resulted in slower degradation of endogenous PLK2 compared with DMSO treatment (Fig. 5B).

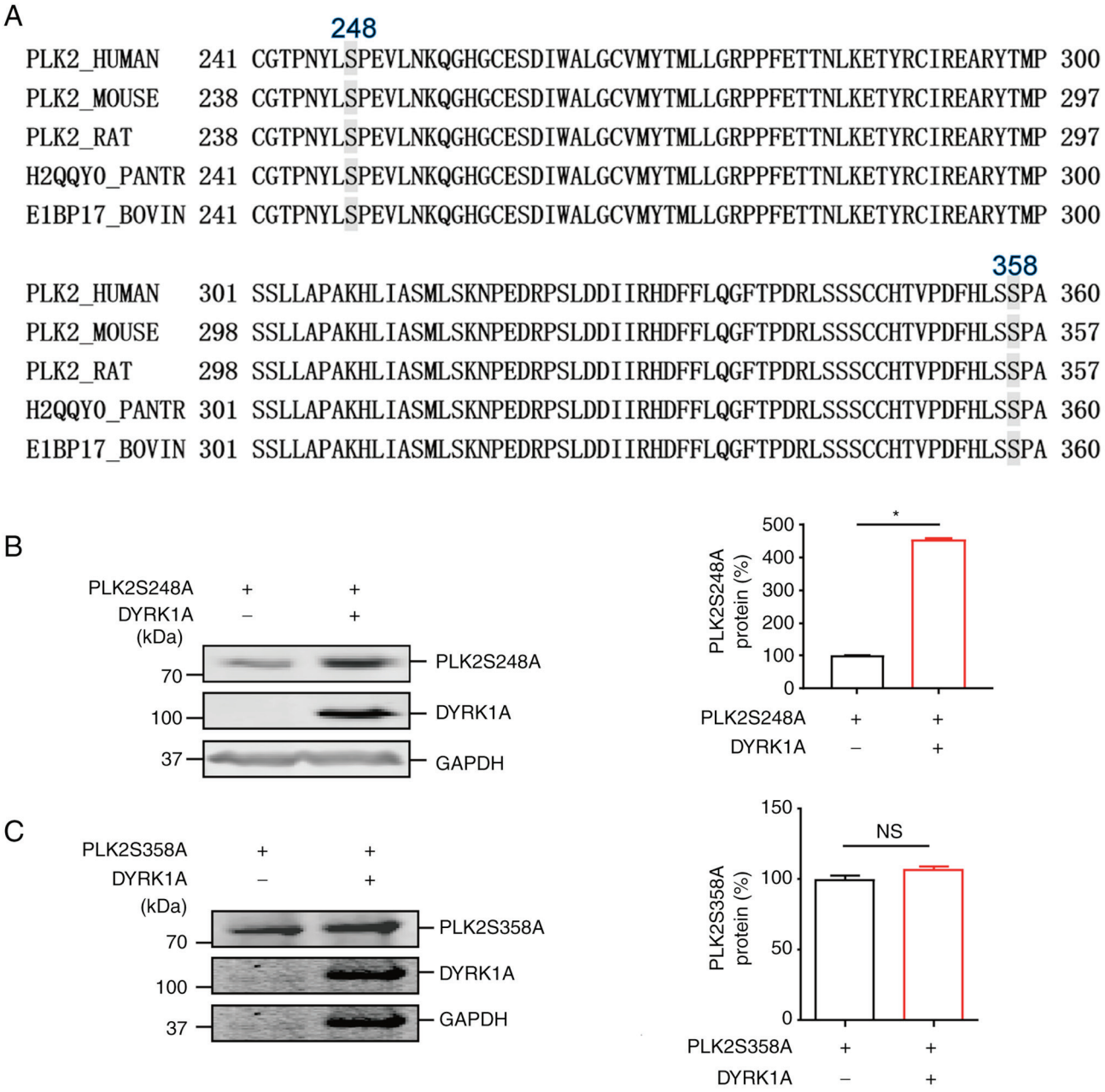

Figure 4. Identification of phosphorylation sites in PLK2 by DYRK1A. (A) Putative phosphorylation sites on PLK2 induced by DYRK1A among different species. (B) 293 cells were transfected with PLK2S248A with the DYRK1A expression vector or the control vector. PLK2 protein expression was detected by WB (n=3). (C) 293 cells were transfected with PLK2 S358A with the DYRK1A expression vector or the control vector. PLK2 protein expression was detected by WB (n=3). *P<0.05. PLK2, polo-like kinase 2; DYRK1A, dual specificity tyrosine-phosphorylation-regulated kinase 1A; WB, western blotting; NS, not significant.

Taken together, the findings of the present study demonstrated that DYRK1A-mediated phosphorylation may increase PLK2 protein stability *in vitro*.

Enhancement of PLK2 kinase activity by DYRK1A. PLK2 kinase activity is vitally crucial for substrate phosphorylation. To investigate whether PLK2 kinase activity was impacted by DYRK1A, PLK2 kinase activity was examined by detecting α-synuclein Ser129 phosphorylation. α-synuclein is widely acknowledged as a specific substrate of PLK2. PLK2 overexpression markedly increases phosphorylation of α-synuclein at Ser129 and promotes abnormal aggregation of α-synuclein (31,32). Hence, α-synuclein Ser129 phosphorylation could be used as an indicator of PLK2 kinase activity. Notably, both DYRK1A and PLK2 increased α-synuclein accumulation compared with the control (Fig. 6A). Consistent with the previous studies (31,32), PLK2 robustly induces α-synuclein Ser129 phosphorylation. However, DYRK1A introduction alone was not able to induce α-synuclein Ser129 phosphorylation (Fig. 6A). Notably, α-synuclein Ser129 phosphorylation was significantly increased in the presence of both PLK2 and DYRK1A compared with PLK2 alone (Fig. 6B). This result suggested that the increase in α-synuclein Ser129 phosphorylation may be attributed to the enhancement of PLK2 activity induced by DYRK1A. Further analysis using phosphorylation-null mutant PLK2 S358A and phosphorylation-mimicking

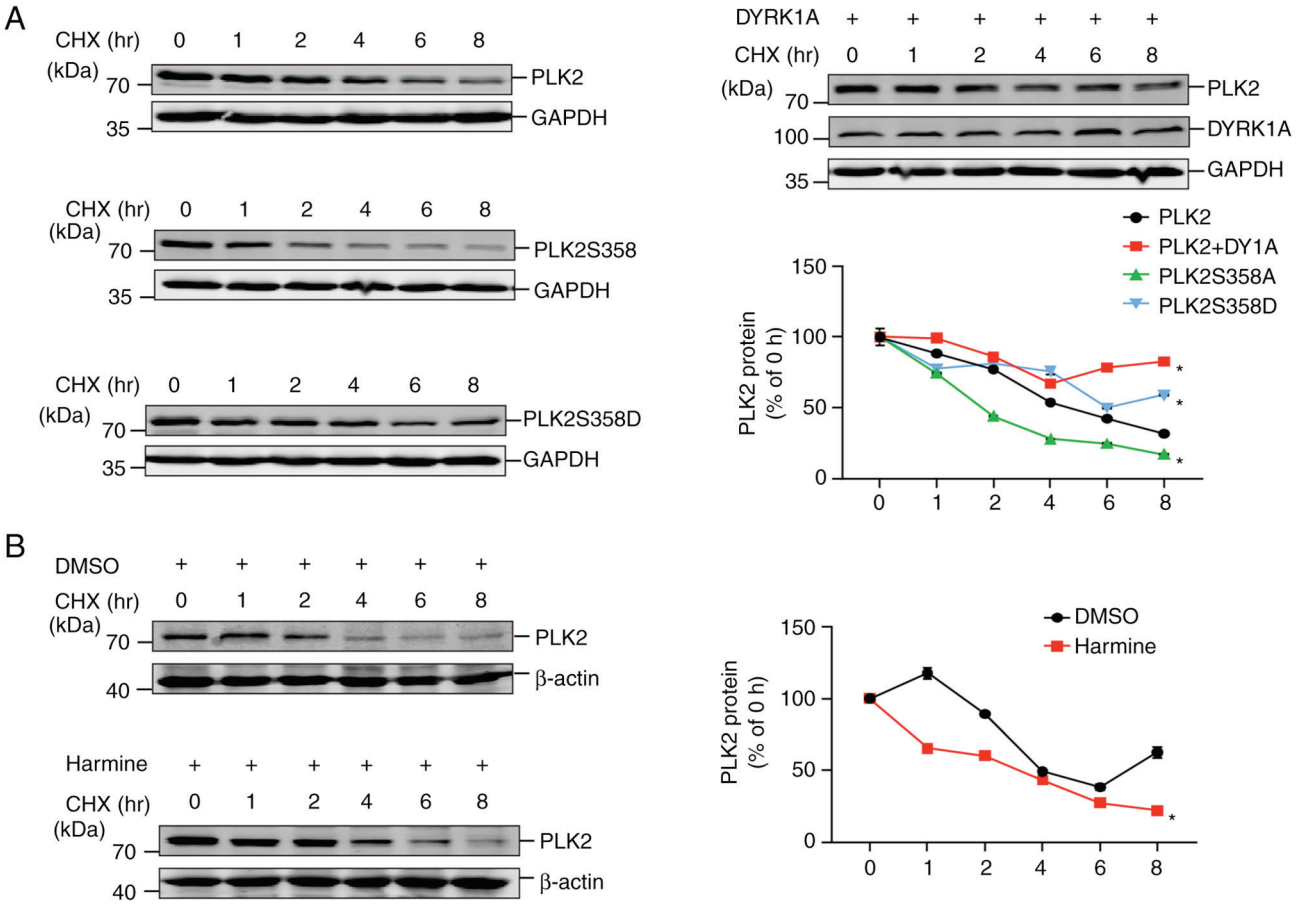

Figure 5. Phosphorylation at Ser358 increases PLK2 protein stability. (A) Degradation of PLK2 was measured by CHX pulse-chase assay, which was performed on 293 cells transfected with PLK2, PLK2 together with DYRK1A, PLK2 S358A, and PLK2 S358D (n=3). (B) Harmine was applied to evaluate the effect of DYRK1A on PLK2 protein degradation. 293 cells were transfected with PLK2. A total of 24 h after transfection, harmine was added to the cell culture media at 10 μM for another 24 h. A CHX pulse-chase assay was then performed (n=3). *P<0.05. PLK2, polo-like kinase 2; CHX, cycloheximide; DYRK1A, dual specificity tyrosine-phosphorylation-regulated kinase 1A.

mutant PLK2 S358D was applied for comparison. Compared with wild-type PLK2, PLK2 S358A had significantly reduced α-synuclein Ser129 phosphorylation. Conversely, PLK2 S358D significantly elevated α-synuclein Ser129 phosphorylation (Fig. 6C). Taken together, these data demonstrated that Ser358 of PLK2 is critical for PLK2 kinase activity and can be modulated by DYRK1A.

DYRK1A-mediated phosphorylation attenuates proliferation and migration/invasion in GBM cells. Previous studies revealed that PLK2 and DYRK1A are highly correlated with GBM malignancy (7,33). Whether their interaction contributes to GBM properties has yet to be uncovered. In the present study, *in vitro* cell viability assays as well as colony formation assays were first performed on U87MG and U251MG stable cells. The results indicated that PLK2 introduction significantly impaired cell viability, while PLK2 silencing had the opposite effect. The introduction of PLK2 together with DYRK1A further suppressed cell viability compared with introducing PLK2 alone (Fig. 7A). Moreover, PLK2 overexpression significantly decreased cell self-renewal, which was even weakened in the presence of DYRK1A in U251MG cells (Fig. 7B). It is noteworthy that U87MG cells are incapable of growing into colonies with such few cells for colony formation assay. U87MG cells can grow colonies only if cell confluency reaches 50% or more. Migration and invasion are essential processes in GBM progression; thus, it was then investigated whether the interaction of PLK2 and DYRK1A affects these processes in GBM cells. The wound healing assay results demonstrated that the migratory ability of U87MG and U251MG cells was significantly decreased upon PLK2 overexpression and further attenuated in the presence of PLK2 together with DYRK1A (Fig. 7C). Additionally, the invasion potential of both cell lines was determined by the Transwell invasion assay. DYRK1A significantly enhanced the suppression of invasion induced by PLK2 in U87MG and U251MG cells (Fig. 7D). Collectively, these data indicated the potential roles of DYRK1A-mediated PLK2 phosphorylation in regulating glioma cell malignancy (Fig. 8).

Discussion

The involvement of PLKs in various cancer types has been extensively studied, including their potential as therapeutic targets in GBM, where PLK2 has been identified as a novel prognostic biomarker (6). Hypermethylation of PLK2 has been implicated in GBM prognosis (34). PLK2 commonly serves as a tumor suppressor, and the expression of PLK2 is frequently

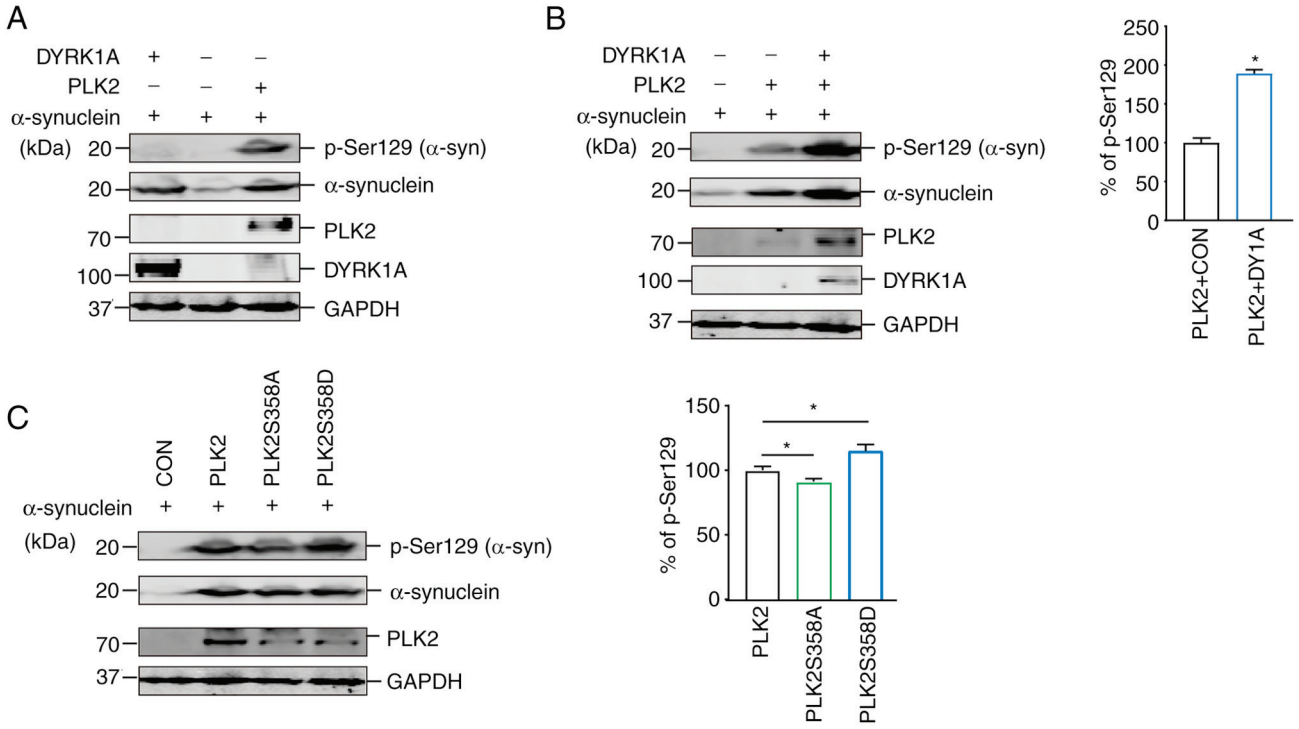

Figure 6. Enhancement of PLK2 kinase activity by DYRK1A. (A) 293 cells were transfected with α-synuclein expression vector together with PLK2 or DYRK1A expression vector. α-synuclein, α-synuclein S129, PLK2 and DYRK1A protein expression was detected by WB. (n=3). (B) 293 cells were transfected with α-synuclein expression vector together with PLK2 alone or both PLK2 and DYRK1A expression vectors. α-synuclein, α-synuclein S129, PLK2, and DYRK1A protein expression was detected by WB (n=3). (C) 293 cells were transfected with α-synuclein expression vector together with PLK2, PLK2S358A or PLK2S358D expression vectors. α-synuclein, α-synuclein S129 and PLK2 protein expression were detected by WB (n=3). *P<0.05. PLK2, polo-like kinase 2; DYRK1A, dual specificity tyrosine-phosphorylation-regulated kinase 1A; WB, western blotting.

lower in multiple types of cancer, including GBM. Strikingly, it was identified that a high level of PLK2 was still positively correlated with poor prognosis. These results indicated that uncharacterized regulatory mechanisms may be involved.

The tumorigenic role of PLK2 is intricate and multifaceted. PLK2 dysregulation has been observed in various cancer types and is considered to play pivotal roles in cancer pathogenesis. For instance, partial or complete loss of PLK2 expression commonly occurs in colorectal carcinomas and impacts mTOR signaling (35). Silencing PLK2 leads to increased cell proliferation and decreased apoptosis in gastric cancer cells (36). PLK2 mRNA and protein expression are simultaneously low in hepatocellular carcinoma and are positively correlated with patient OS (37). In addition, PLK2 is hypermethylated in a high percentage of patients with multiple myeloma and B-cell lymphoma (38). Of note, PLK2 expression is exceedingly suppressed in GBM samples, particularly in temozolomide-resistant GBM. Reduced PLK2 expression enhances temozolomide resistance in GBM by activating Notch signaling. Meanwhile, upregulation of PLK2 decreased GBM cell malignancy (7), which is in line with the present results. In the present study, it was found that PLK2 could interact with DYRK1A and be phosphorylated by it *in vitro*. A previous study showed that four phosphorylation sites, including Ser497, Ser588, Tyr590 and Ser299, affect PLK2 protein stability (25). It was observed that DYRK1A-mediated phosphorylation increased PLK2 protein levels by decelerating its degradation, further addressing the critical role of PLK2 phosphorylation in PLK2 protein stability. Introduction of DYRK1A in the presence of PLK2 further attenuates proliferation, migration and invasion of GBM cells *in vitro*, underscoring the substantial contribution of DYRK1A-mediated PLK2 phosphorylation in GBM cell malignancy.

The functional importance of PLK2 kinase activity has been extensively studied. PLK2 has been found to phosphorylate PLK1 at Ser-137, which is sufficient to mediate the survival signal in colon cancer cells, highlighting the important role of PLK2 kinase activity in cell growth (39). In addition, PLK2 phosphorylates CPAP at S589 and S595, impacting procentriole formation during the centrosome cycle (40). In the central nervous system, PLK2 phosphorylates alpha-synuclein at Ser129, rendering alpha-synuclein one of the major substrates of PLK2 (41). In the present study, it was revealed that the S358A mutant of PLK2 has no effect on alpha-synuclein Ser129 phosphorylation, whereas the phospho-mimicking mutant PLK2S358D enhances alpha-synuclein Ser129 phosphorylation. These results demonstrated that the phosphorylation of Ser358 induced by DYRK1A tightly regulates PLK2 kinase activity.

The role of DYRK1A in the pathogenesis of multiple types of cancer is controversial. DYRK1A plays a tumor-promoting role in acute megakaryocytic leukemia in Down's syndrome models (42), B-cell acute lymphoblastic leukemia (14), neuroblastoma (43), pancreatic ductal adenocarcinoma (44), ovarian cancer (45), non-small cell lung cancer (46,47), bladder cancer (48) and head and neck squamous cell carcinoma (49). Conversely, DYRK1A exerts a tumor suppressive effect in acute myeloid leukemia (50). Notably, DYRK1A appears to act as a

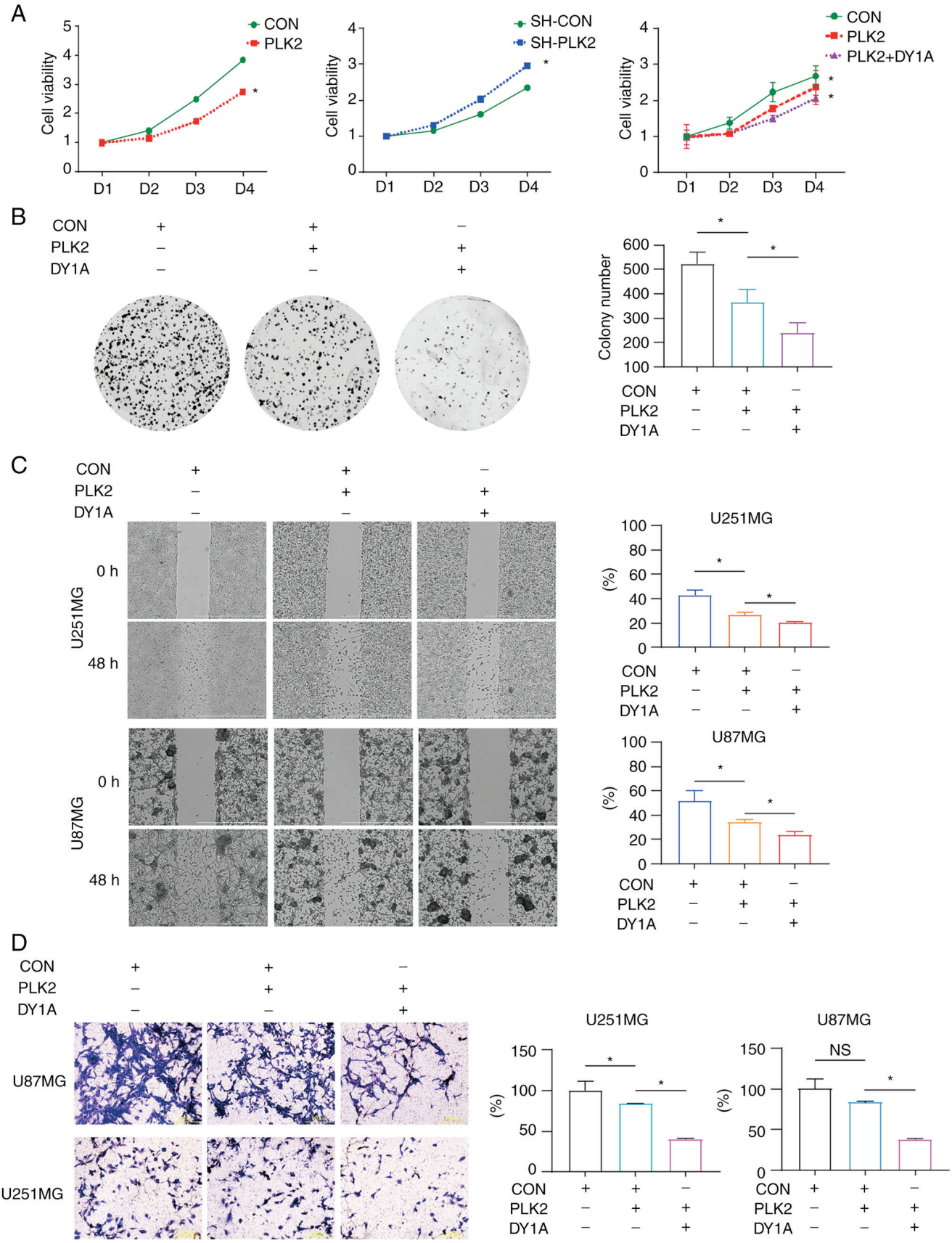

Figure 7. DYRK1A-mediated phosphorylation attenuates proliferation and migration/invasion in glioblastoma cells. (A) Cell viability of U87MG cells infected by lentivirus carrying the gene of interest was measured by Cell Counting Kit-8 assay (n=3). (B) Proliferation of U251MG cells infected with lentivirus carrying PLK2, DYRK1A and the control vector was measured by colony formation assay (n=3). (C) The migration capability of PLK2/DYRK1A was measured by wound healing assay of U87MG and U251MG cells infected with lentivirus carrying PLK2, DYRK1A and the control vector (Scale bars, 1,000 μm). Quantitative analysis of the wound healing assay (n=3). (D) Invasion capability was measured by Transwell invasion assay of U87MG and U251MG cells infected with lentivirus carrying PLK2, DYRK1A and the control vector. Quantitative analysis of the wound healing assay (n=3). *P<0.05. DYRK1A, dual specificity tyrosine-phosphorylation-regulated kinase 1A; PLK2, polo-like kinase 2; NS, not significant.

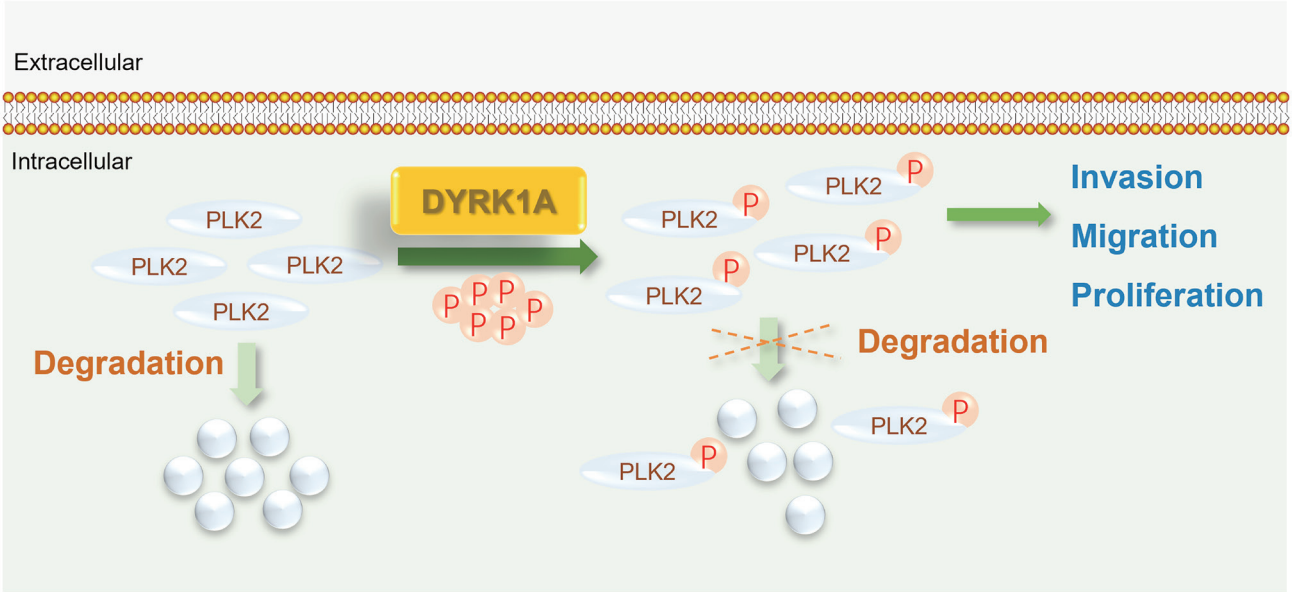

Figure 8. Diagram delineating the role of DYRK1A-mediated PLK2 phosphorylation in glioblastoma cells. DYRK1A, dual specificity tyrosine-phosphorylation-regulated kinase 1A; PLK2, polo-like kinase 2.

double-edge kinase in GBM and osteosarcoma (11,51-54). In the present study, differential expression of DYRK1A was not observed in GBM. Nevertheless, an antitumoral capacity of the DYRK1A/PLK2 axis in regulating the biological processes of GBM cells was revealed. DYRK1A enhances PLK2-induced cell growth inhibition by phosphorylating PLK2 at Ser358, a critical site responsible for kinase activity. DYRK1A-mediated PLK2 phosphorylation attenuates cell migration and invasion. Of note, introduction of DYRK1A alone may facilitate GBM cell growth (data not shown). However, it was observed that the co-expression of PLK2 and DYRK1A suppresses tumor cell malignancy. Numerous selective DYRK inhibitors for cancers, including GBM, have been described in previous studies (11,51,55,56). None of the DYRK1A inhibitors have been approved for clinical use in GBM, although certain of them show promising effects in clinical studies (51,57). Therefore, the present study enriched the possible mechanism of DYRK1A in GBM pathogenesis.

Further investigation is required to fully comprehend the potential therapeutic applications of PLK2. PLK2-mediated TAp73 phosphorylation prevents TAp73 activity, which confers an invasive phenotype through activation of POSTN (58,59). Nevertheless, how the DYRK1A/PLK2/TAp73 axis functions in GBM remains unknown. In addition, the potential damage to healthy brain tissue caused by radiation therapy against GBM, such as inflammation and necrosis, is a major concern. Radiation-induced necrosis has been reported to affect over 30% of patients with GBM (60-62). A previous study has shown that PLK2-mediated phosphorylation and translocation of Nrf2 activates anti-inflammatory effects via p53/Plk2/p21^{cip1} signaling in acute kidney injury (63). Nrf2 is a critical regulatory factor that helps GBM tumors maintain low immunogenicity and antiapoptotic proliferative phenotypic characteristics (64). Therefore, it is worthwhile to investigate whether the DYRK1A/PLK2/Nrf axis is involved in GBM immunogenicity regulation.

Acknowledgements

The authors would like to thank the biological imaging facility of Shandong University for their support in immunofluorescence image acquisition and analysis. The authors would also like to thank Dr Xiulian Sun (Shandong University, China) for generously providing them with the pCMV6-entry-DYRK1A vector.

Funding

The present study was supported by the Natural Science Foundation of Shandong (grant no. ZR2022MH313).

Availability of data and materials

All data generated or analyzed during this study are included in this published article. PLK2 expression in multiple cancers is available on TIMER2.0 database(http://timer.cistrome.org/).

Authors' contributions

ST and PW conceived and designed the experiments. ST and JZ performed the experiments. ST and PW performed the bioinformatics and data analysis. PW reviewed and revised the manuscript. All authors read and approved the final manuscript. ST and PW confirm the authenticity of all the raw data.

Ethics approval and consent to participate

Not applicable.

Patient consent for publication

Not applicable.

Competing interests

The authors declare that they have no competing interests.

References

1. Louis DN, Holland EC and Cairncross JG: Glioma classification: A molecular reappraisal. Am J Pathol 159: 779-786, 2001.
2. Janjua TI, Rewatkar P, Ahmed-Cox A, Saeed I, Mansfeld FM, Kulshreshtha R, Kumeria T, Ziegler DS, Kavallaris M, Mazzieri R and Popat A: Frontiers in the treatment of glioblastoma: Past, present and emerging. Adv Drug Deliv Rev 171: 108-138, 2021.
3. Bhullar KS, Lagarón NO, McGowan EM, Parmar I, Jha A, Hubbard BP and Rupasinghe HPV: Kinase-targeted cancer therapies: Progress, challenges and future directions. Mol Cancer 17: 48, 2018.
4. Shah NP, Tran C, Lee FY, Chen P, Norris D and Sawyers CL: Overriding imatinib resistance with a novel ABL kinase inhibitor. Science 305: 399-401, 2004.
5. Lombardo LJ, Lee FY, Chen P, Norris D, Barrish JC, Behnia K, Castaneda S, Cornelius LA, Das J, Doweyko AM, *et al*: Discovery of N-(2-chloro-6-methyl-phenyl)-2-(6-(4-(2-hydroxyethyl)-piperazin-1-yl)-2-methylpyrimidin-4-ylamino)thiazole-5-carboxamide (BMS-354825), a dual Src/Abl kinase inhibitor with potent antitumor activity in preclinical assays. J Med Chem 47: 6658-6661, 2004.
6. Ding Y, Liu H, Zhang C, Bao Z and Yu S: Polo-like kinases as potential targets and PLK2 as a novel biomarker for the prognosis of human glioblastoma. Aging (Albany NY) 14: 2320-2334, 2022.
7. Alafate W, Xu D, Wu W, Xiang J, Ma X, Xie W, Bai X, Wang M and Wang J: Loss of PLK2 induces acquired resistance to temozolomide in GBM via activation of notch signaling. J Exp Clin Cancer Res 39: 239, 2020.
8. Boni J, Rubio-Perez C, López-Bigas N, Fillat C and de la Luna S: The DYRK family of kinases in cancer: Molecular functions and therapeutic opportunities. Cancers (Basel) 12: 2106, 2020.
9. Li Y, Xie X, Jie Z, Zhu L, Yang JY, Ko CJ, Gao T, Jain A, Jung SY, Baran N, *et al*: DYRK1a mediates BAFF-induced noncanonical NF-κB activation to promote autoimmunity and B-cell leukemogenesis. Blood 138: 2360-2371, 2021.
10. Li YL, Zhang MM, Wu LW, Liu YH, Zhang ZY, Zeng LH, Lin NM and Zhang C: DYRK1A reinforces epithelial-mesenchymal transition and metastasis of hepatocellular carcinoma via cooperatively activating STAT3 and SMAD. J Biomed Sci 29: 34, 2022.
11. Recasens A, Humphrey SJ, Ellis M, Hoque M, Abbassi RH, Chen B, Longworth M, Needham EJ, James DE, Johns TG, *et al*: Global phosphoproteomics reveals DYRK1A regulates CDK1 activity in glioblastoma cells. Cell Death Discov 7: 81, 2021.
12. Kaltheuner IH, Anand K, Moecking J, Düster R, Wang J, Gray NS and Geyer M: Abemaciclib is a potent inhibitor of DYRK1A and HIP kinases involved in transcriptional regulation. Nat Commun 12: 6607, 2021.
13. Ehe BK, Lamson DR, Tarpley M, Onyenwoke RU, Graves LM and Williams KP: Identification of a DYRK1A-mediated phosphorylation site within the nuclear localization sequence of the hedgehog transcription factor GLI1. Biochem Biophys Res Commun 491: 767-772, 2017.
14. Bhansali RS, Rammohan M, Lee P, Laurent AP, Wen Q, Suraneni P, Yip BH, Tsai YC, Jenni S, Bornhauser B, *et al*: DYRK1A regulates B cell acute lymphoblastic leukemia through phosphorylation of FOXO1 and STAT3. J Clin Invest 131: e135937, 2021.
15. Choi HK and Chung KC: Dyrk1A positively stimulates ASK1-JNK signaling pathway during apoptotic cell death. Exp Neurobiol 20: 35-44, 2011.
16. Madhavan S, Zenklusen JC, Kotliarov Y, Sahni H, Fine HA and Buetow K: Rembrandt: Helping personalized medicine become a reality through integrative translational research. Mol Cancer Res 7: 157-167, 2009.
17. Gravendeel LAM, Kouwenhoven MCM, Gevaert O, de Rooi JJ, Stubbs AP, Duijm JE, Daemen A, Bleeker FE, Bralten LB, Kloosterhof NK, *et al*: Intrinsic gene expression profiles of gliomas are a better predictor of survival than histology. Cancer Res 69: 9065-9072, 2009.
18. Sun L, Hui AM, Su Q, Vortmeyer A, Kotliarov Y, Pastorino S, Passaniti A, Menon J, Walling J, Bailey R, *et al*: Neuronal and glioma-derived stem cell factor induces angiogenesis within the brain. Cancer Cell 9: 287-300, 2006.
19. Tan S, Spear R, Zhao J, Sun X and Wang P: Comprehensive characterization of a novel E3-related gene signature with implications in prognosis and immunotherapy of low-grade gliomas. Front Genet 13: 905047, 2022.
20. Alafate W, Li X, Zuo J, Zhang H, Xiang J, Wu W, Xie W, Bai X, Wang M and Wang J: Elevation of CXCL1 indicates poor prognosis and radioresistance by inducing mesenchymal transition in glioblastoma. CNS Neurosci Ther 26: 475-485, 2020.
21. Liu Q, Tang Y, Chen L, Liu N, Lang F, Liu H, Wang P and Sun X: E3 ligase SCFβTrCP-induced DYRK1A protein degradation is essential for cell cycle progression in HEK293 cells. J Biol Chem 291: 26399-26409, 2016.
22. Wang P, Zhao J and Sun X: DYRK1A phosphorylates MEF2D and decreases its transcriptional activity. J Cell Mol Med 25: 6082-6093, 2021.
23. Livak KJ and Schmittgen TD: Analysis of relative gene expression data using real-time quantitative PCR and the 2(-Delta Delta C(T)) method. Methods 25: 402-408, 2001.
24. Franken NAP, Rodermond HM, Stap J, Haveman J and van Bree C: Clonogenic assay of cells in vitro. Nat Protoc 1: 2315-2319, 2006.
25. Rozeboom AM and Pak DTS: Identification and functional characterization of polo-like kinase 2 autoregulatory sites. Neuroscience 202: 147-157, 2012.
26. Himpel S, Panzer P, Eirmbter K, Czajkowska H, Sayed M, Packman LC, Blundell T, Kentrup H, Grötzinger J, Joost HG and Becker W: Identification of the autophosphorylation sites and characterization of their effects in the protein kinase DYRK1A. Biochem J 359: 497-505, 2001.
27. Himpel S, Tegge W, Frank R, Leder S, Joost HG and Becker W: Specificity determinants of substrate recognition by the protein kinase DYRK1A. J Biol Chem 275: 2431-2438, 2000.
28. Ma S, Liu MA, Yuan YLO and Erikson RL: The serum-inducible protein kinase Snk is a G1 phase polo-like kinase that is inhibited by the calcium- and integrin-binding protein CIB. Mol Cancer Res 1: 376-384, 2003.
29. Göckler N, Jofre G, Papadopoulos C, Soppa U, Tejedor FJ and Becker W: Harmine specifically inhibits protein kinase DYRK1A and interferes with neurite formation. FEBS J 276: 6324-6337, 2009.
30. Kumar K, Wang P, Sanchez R, Swartz EA, Stewart AF and DeVita RJ: Development of kinase-selective, harmine-based DYRK1A inhibitors that induce pancreatic human β-cell proliferation. J Med Chem 61: 7687-7699, 2018.
31. Mbefo MK, Paleologou KE, Boucharaba A, Oueslati A, Schell H, Fournier M, Olschewski D, Yin G, Zweckstetter M, Masliah E, *et al*: Phosphorylation of synucleins by members of the polo-like kinase family. J Biol Chem 285: 2807-2822, 2010.
32. Waxman EA and Giasson BI: Characterization of kinases involved in the phosphorylation of aggregated α-synuclein. J Neurosci Res 89: 231-247, 2011.
33. Liu H, Sun Q, Chen S, Chen L, Jia W, Zhao J and Sun X: DYRK1A activates NFATC1 to increase glioblastoma migration. Cancer Med 10: 6416-6427, 2021.
34. Xia X, Cao F, Yuan X, Zhang Q, Chen W, Yu Y, Xiao H, Han C and Yao S: Low expression or hypermethylation of PLK2 might predict favorable prognosis for patients with glioblastoma multiforme. PeerJ 7: e7974, 2019.
35. Matthew EM, Yang Z, Peri S, Andrake M, Dunbrack R, Ross E and El-Deiry WS: Plk2 loss commonly occurs in colorectal carcinomas but not adenomas: Relationship to mTOR signaling. Neoplasia 20: 244-255, 2018.
36. Liu LY, Wang W, Zhao LY, Guo B, Yang J, Zhao XG, Song TS, Huang C and Xu JR: Silencing of polo-like kinase 2 increases cell proliferation and decreases apoptosis in SGC-7901 gastric cancer cells. Mol Med Rep 11: 3033-3038, 2015.
37. Pellegrino R, Calvisi DF, Ladu S, Ehemann V, Staniscia T, Evert M, Dombrowski F, Schirmacher P and Longerich T: Oncogenic and tumor suppressive roles of polo-like kinases in human hepatocellular carcinoma. Hepatology 51: 857-868, 2010.
38. Benetatos L, Dasoula A, Hatzimichael E, Syed N, Voukelatou M, Dranitsaris G, Bourantas KL and Crook T: Polo-like kinase 2 (SNK/PLK2) is a novel epigenetically regulated gene in acute myeloid leukemia and myelodysplastic syndromes: Genetic and epigenetic interactions. Ann Hematol 90: 1037-1045, 2011.

39. Matsumoto T, Wang P, Ma W, Sung HJ, Matoba S and Hwang PM: Polo-like kinases mediate cell survival in mitochondrial dysfunction. Proc Natl Acad Sci USA 106: 14542-14546, 2009.
40. Chang J, Cizmecioglu O, Hoffmann I and Rhee K: PLK2 phosphorylation is critical for CPAP function in procentriole formation during the centrosome cycle. EMBO J 29: 2395-2406, 2010.
41. Inglis KJ, Chereau D, Brigham EF, Chiou SS, Schöbel S, Frigon NL, Yu M, Caccavello RJ, Nelson S, Motter R, *et al*: Polo-like kinase 2 (PLK2) phosphorylates alpha-synuclein at serine 129 in central nervous system. J Biol Chem 284: 2598-2602, 2009.
42. Malinge S, Bliss-Moreau M, Kirsammer G, Diebold L, Chlon T, Gurbuxani S and Crispino JD: Increased dosage of the chromosome 21 ortholog Dyrk1a promotes megakaryoblastic leukemia in a murine model of down syndrome. J Clin Invest 122: 948-962, 2012.
43. Soppa U, Schumacher J, Florencio Ortiz V, Pasqualon T, Tejedor FJ and Becker W: The down syndrome-related protein kinase DYRK1A phosphorylates p27(Kip1) and cyclin D1 and induces cell cycle exit and neuronal differentiation. Cell Cycle 13: 2084-2100, 2014.
44. Luna J, Boni J, Cuatrecasas M, Bofill-De Ros X, Núñez-Manchón E, Gironella M, Vaquero EC, Arbones ML, de la Luna S and Fillat C: DYRK1A modulates c-MET in pancreatic ductal adenocarcinoma to drive tumour growth. Gut 68: 1465-1476, 2019.
45. MacDonald J, Ramos-Valdes Y, Perampalam P, Litovchick L, DiMattia GE and Dick FA: A systematic analysis of negative growth control implicates the DREAM complex in cancer cell dormancy. Mol Cancer Res 15: 371-381, 2017.
46. Li Y, Zhou D, Xu S, Rao M, Zhang Z, Wu L, Zhang C and Lin N: DYRK1A suppression restrains Mcl-1 expression and sensitizes NSCLC cells to Bcl-2 inhibitors. Cancer Biol Med 17: 387-400, 2020.
47. Li YL, Ding K, Hu X, Wu LW, Zhou DM, Rao MJ, Lin NM and Zhang C: DYRK1A inhibition suppresses STAT3/EGFR/Met signalling and sensitizes EGFR wild-type NSCLC cells to AZD9291. J Cell Mol Med 23: 7427-7437, 2019.
48. Kottakis F, Polytarchou C, Foltopoulou P, Sanidas I, Kampranis SC and Tsichlis PN: FGF-2 regulates cell proliferation, migration, and angiogenesis through an NDY1/KDM2B-miR-101-EZH2 pathway. Mol Cell 43: 285-298, 2011.
49. Martin CE, Nguyen A, Kang MK, Kim RH, Park NH and Shin KH: DYRK1A is required for maintenance of cancer stemness, contributing to tumorigenic potential in oral/oropharyngeal squamous cell carcinoma. Exp Cell Res 405: 112656, 2021.
50. Guard SE, Poss ZC, Ebmeier CC, Pagratis M, Simpson H, Taatjes DJ and Old WM: The nuclear interactome of DYRK1A reveals a functional role in DNA damage repair. Sci Rep 9: 6539, 2019.
51. Pozo N, Zahonero C, Fernández P, Liñares JM, Ayuso A, Hagiwara M, Pérez A, Ricoy JR, Hernández-Laín A, Sepúlveda JM and Sánchez-Gómez P: Inhibition of DYRK1A destabilizes EGFR and reduces EGFR-dependent glioblastoma growth. J Clin Invest 123: 2475-2487, 2013.
52. Lee SB, Frattini V, Bansal M, Castano AM, Sherman D, Hutchinson K, Bruce JN, Califano A, Liu G, Cardozo T, *et al*: An ID2-dependent mechanism for VHL inactivation in cancer. Nature 529: 172-177, 2016.
53. Litovchick L, Florens LA, Swanson SK, Washburn MP and DeCaprio JA: DYRK1A protein kinase promotes quiescence and senescence through DREAM complex assembly. Genes Dev 25: 801-813, 2011.
54. Guo X, Williams JG, Schug TT and Li X: DYRK1A and DYRK3 promote cell survival through phosphorylation and activation of SIRT1. J Biol Chem 285: 13223-13232, 2010.
55. Zhang L, Li D and Yu S: Pharmacological effects of harmine and its derivatives: A review. Arch Pharm Res 43: 1259-1275, 2020.
56. Lee Walmsley D, Murray JB, Dokurno P, Massey AJ, Benwell K, Fiumana A, Foloppe N, Ray S, Smith J, Surgenor AE, *et al*: Fragment-derived selective inhibitors of dual-specificity kinases DYRK1A and DYRK1B. J Med Chem 64: 8971-8991, 2021.
57. Zhou Q, Reekie TA, Abbassi RH, Venkata DI, Font JS, Ryan RM, Rendina LM, Munoz L and Kassiou M: Flexible analogues of azaindole DYRK1A inhibitors elicit cytotoxicity in glioblastoma cells*. Aust J Chem 71: 789-797, 2018.
58. Hu ZB, Liao XH, Xu ZY, Yang X, Dong C, Jin AM and Lu H: PLK2 phosphorylates and inhibits enriched TAp73 in human osteosarcoma cells. Cancer Med 5: 74-87, 2016.
59. Landré V, Antonov A, Knight R and Melino G: p73 promotes glioblastoma cell invasion by directly activating POSTN (periostin) expression. Oncotarget 7: 11785-11802, 2016.
60. Brandes AA, Tosoni A, Spagnolli F, Frezza G, Leonardi M, Calbucci F and Franceschi E: Disease progression or pseudoprogression after concomitant radiochemotherapy treatment: Pitfalls in neurooncology. Neuro Oncol 10: 361-367, 2008.
61. DeAngelis LM, Delattre JY and Posner JB: Radiation-induced dementia in patients cured of brain metastases. Neurology 39: 789-796, 1989.
62. Sheline GE, Wara WM and Smith V: Therapeutic irradiation and brain injury. Int J Radiat Oncol Biol Phys 6: 1215-1228, 1980.
63. Kim DE, Byeon HE, Kim DH, Kim SG and Yim H: Plk2-mediated phosphorylation and translocalization of Nrf2 activates anti-inflammation through p53/Plk2/p21^{cip1} signaling in acute kidney injury. Cell Biol Toxicol: Jul 16, 2022 (Epub ahead of print).
64. Awuah WA, Toufik AR, Yarlagadda R, Mikhailova T, Mehta A, Huang H, Kundu M, Lopes L, Benson S, Mykola L, *et al*: Exploring the role of Nrf2 signaling in glioblastoma multiforme. Discov Oncol 13: 94, 2022.